IEEE Access
Multidisciplinary | Rapid Review | Open Access Journal

Received March 19, 2020, accepted April 3, 2020, date of publication April 7, 2020, date of current version April 30, 2020.

Digital Object Identifier 10.1109/ACCESS.2020.2986280

Enhanced Peak Cancellation With Simplified In-Band Distortion Compensation for Massive MIMO-OFDM

TOMOYA KAGEYAMA[1], (Student Member, IEEE), OSAMU MUTA[2], (Member, IEEE), AND HARIS GACANIN[3], (Senior Member, IEEE)

[1]Graduate School of Information Science and Electrical Engineering, Kyushu University, Fukuoka 8190395, Japan
[2]Center for Japan-Egypt Cooperation in Science and Technology, Kyushu University, Fukuoka 8190395, Japan
[3]Faculty of Electrical Engineering and Information Technologies, RWTH Aachen University, 52074 Aachen, Germany

Corresponding author: Tomoya Kageyama (kageyama@mobcom.ait.kyushu-u.ac.jp)

This work was supported in part by the Japan Society for the Promotion of Science (JSPS) KAKENHI under Grant JP17K06427 and Grant JP17J04710.

ABSTRACT This paper presents an enhanced peak cancellation method with simplified in-band distortion compensation for massive multi-input multi-output (mMIMO) orthogonal frequency division multiplexing (OFDM). The method compensates an in-band distortion due to peak cancellation by utilizing extra transmit antennas, where a compensation signal is designed and transmitted using extra antenna elements so that in-band distortion is canceled at the receiver end. Consequently, deep peak cancellation is possible without degrading bit error rate performance. The proposed method is further extended to non-linear precoded mMIMO-OFDM systems, where the perturbation vector cancellation signal is superimposed on the compensation signal so that the received signal is demodulated without non-linear processing to remove the perturbation vector. Thus, the proposed method does not require the iterative calculation to compensate for an in-band distortion. Our results show the effectiveness of the proposed method in terms of peak-to-average power ratio (PAPR) characteristics, signal to noise and distortion power ratio (SDNR), bit error rate (BER), and throughput in comparison with the state-of-the-art.

INDEX TERMS Massive multiple-input multiple-output (MIMO), orthogonal frequency-division multiplexing (OFDM), peak-to-average power ratio (PAPR).

I. INTRODUCTION

Massive multi-input multi-output with orthogonal frequency division multiplexing (mMIMO-OFDM) is one of the key enablers for future wireless communication systems that achieve higher spectrum efficiency [1], [2]. However, one of the drawbacks in OFDM is high peak-to-average power ratio (PAPR) which may cause non-linear distortion and out-of-band (OoB) radiation at the output of power amplifier. Thus, PAPR reduction for OFDM signal is a challenging issue, and various PAPR reduction methods are investigated [3]–[13].

Recently, PAPR reduction methods for mMIMO-OFDM systems have been proposed [14]–[23], where extra degrees of freedom at mMIMO is utilized to mitigate in-band distortion and consequently improve the PAPR reduction capability. However, works in [14]–[23] require a high computational cost to optimize the precoder to minimize the PAPR, while keeping the orthogonality between spatially multiplexed signals. The authors in [17] have proposed a limiter-based PAPR reduction and its in-band compensation technique utilizing extra antennas. However, this work does not consider the impact of band-limitation filtering to suppress the out-of-band radiation due to non-linear distortion. Thus, PAPR reduction for mMIMO-OFDM signal is a challenging issue which needs a novel solution.

In this paper, we propose an in-band distortion compensation technique that enhances peak cancellation performance for mMIMO-OFDM,[1] where in-band distortion due to peak cancellation is compensated by using an extra spatial degree of freedoms of massive transmit antenna array. The contributions of this paper are summarized as follows:

The associate editor coordinating the review of this manuscript and approving it for publication was Adnan Kavak.

[1]In part, this work was presented at 2015 IEEE International Symposium on Personal Indoor and Mobile Radio Communications [12], [13].

- We propose an enhanced peak cancellation framework with a low-complexity in-band distortion compensation for mMIMO-OFDM. The proposed method employs extra spatial degree of freedom (i.e., extra antenna elements) to compensate in-band distortion without iterative signal processing on the transmitter. An in-band distortion compensation signal is transmitted using extra antenna elements so that in-band distortion due to peak cancellation is canceled at the receiver end. Unlike state-of-the-art, our method allows deep peak cancellation without degrading bit error rate performance even for higher-order modulation such as 64QAM.
- We extend the proposed method to non-linear precoding of mMIMO-OFDM such as Tomlinson Harashima precoding (THP) and vector perturbation (VP), where perturbation vector cancellation signal is superimposed on the in-band distortion compensation signal so that the received signal is demodulated without non-linear processing to remove perturbation vector. In addition, we design a simplified sub-carrier power control technique designed as an equivalent non-linear precoding operation for mMIMO-OFDM with peak cancellation and its in-band distortion compensation.
- Finally, we introduce an adaptive in-band distortion compensation technique that achieves a good trade-off between compensation of in-band distortion and precoding gain in mMIMO-OFDM. Our results show that the proposed adaptive compensation of in-band distortion outperforms the compensation method with full-compensation that need a greater number of extra antennas to compensate for the distortion completely.

II. SYSTEM MODEL

The mMIMO-OFDM system model considered in this paper is illustrated in Fig. 1. N_t, N_r, M, and N_{ex} denote the number of transmit antennas at the base station, the number of receive antennas per user, the number of users, and the number of extra antennas, respectively. We consider mMIMO-OFDM systems with linear precoding and non-linear precoding as in Figs. 1(a) and (b), respectively. The receiver side is also illustrated in Fig. 1(c). Note that the proposed system does not require additional processing at the receiver side and thus the receiver configuration is the same for both linear and non-linear cases. Adaptive peak cancellation [12], [13] is adopted at each antenna to suppress peak amplitude below a given threshold level.

The correlated channel matrix $\tilde{H}^l \in \mathbb{C}^{N_r \times N_t}$ is given as

$$\tilde{H}^{(l,m)} = R_r H^{(l,m)} R_t, \tag{1}$$

where $H^{(l,m)} \in \mathbb{C}^{N_r \times N_t}$ denotes the uncorrelated channel matrix for m-th user at l-th subcarrier ($l = 0, \ldots, L-1$) defined as

$$H^{(l,m)} = \begin{bmatrix} H_{11}^{(l,m)} & \cdots & H_{1N_t}^{(l,m)} \\ \vdots & \ddots & \vdots \\ H_{N_r1}^{(l,m)} & \cdots & H_{N_rN_t}^{(l,m)} \end{bmatrix}, \tag{2}$$

where L is the number of subcarriers. Here, $R_t \in \mathbb{R}^{N_t \times N_t}$ and $R_r \in \mathbb{R}^{N_r \times N_r}$ denote the correlation matrix at the base station (BS) and at user equipments (UEs), respectively [26]. We assume that spatial correlation matrix is same among all subcarriers and for all users as follows.

$$R_t = \begin{bmatrix} \rho_{11}^t & \cdots & \rho_{1N_t}^t \\ \vdots & \ddots & \vdots \\ \rho_{N_t1}^t & \cdots & \rho_{N_tN_t}^t \end{bmatrix}, \tag{3}$$

$$R_r = \begin{bmatrix} \rho_{11}^r & \cdots & \rho_{1N_r}^r \\ \vdots & \ddots & \vdots \\ \rho_{N_r1}^r & \cdots & \rho_{N_rN_r}^r \end{bmatrix}, \tag{4}$$

where ρ_{ij}^t and ρ_{ij}^r are correlation factor between i-th antenna and j-th antenna at the BS and UEs, respectively.

$$\rho_{i,j}^t = \exp\left(-\frac{|i-j|}{\beta_t}\right), \quad \rho_{i,j}^r = \exp\left(-\frac{|i-j|}{\beta_r}\right), \tag{5}$$

where β_t and β_r are the parameters that take a value between 0 and 1. Hence, the concatenated channel matrix at l-th subcarrier $H^l \in \mathbb{C}^{MN_r \times N_t}$ is given as

$$H^l = [\tilde{H}^{(l,1)} \ldots \tilde{H}^{(l,m)} \ldots \tilde{H}^{(l,M)}]^T, \tag{6}$$

where m denotes the user index.

For linear precoding case (Fig. 1(a)), let $s^{(l,m)} \in \mathbb{C}^{N_s \times 1}$ denotes the transmitted QAM symbol vector for m-th user at l-th subcarrier, where N_s is the number of streams.

$$s^{(l,m)} = [s_1^{(l,m)}, s_2^{(l,m)}, \ldots, s_{N_s}^{(l,m)}], \tag{7}$$

In this paper we assume $N_s = N_r$. Let $s^l \in \mathbb{C}^{MN_s \times 1}$ denote the concatenated transmitted QAM symbol vector given by

$$\begin{aligned} s^l &= [s^{(l,1)} s^{(l,2)} \ldots s^{(l,M)}]^T \\ &\equiv [\bar{s}_1^l, \bar{s}_2^l, \ldots, \bar{s}_j^l, \ldots, \bar{s}_{MNs}^l]^T, \end{aligned} \tag{8}$$

where superscript T indicates the transpose operation. Let $W^l \in \mathbb{C}^{N_t \times MN_s}$ denote the precoding weight at l-th subcarrier. The transmit signal at l-th subcarrier $x^l \in \mathbb{C}^{N_t \times 1}$ is expressed as

$$x^l = P_t W^l s^l, \tag{9}$$

where P_t is the normalization factor of the transmit power. The received signal at l-th subcarrier $y^l \in \mathbb{C}^{MN_s \times 1}$ is given as

$$\begin{aligned} y^l &= H^l x^l + n^l \\ &= P_t H^l W^l s^l + n^l, \end{aligned} \tag{10}$$

where $n^l \in \mathbb{C}^{MN_s \times 1}$ denotes additive white Gaussian noise (AWGN) vector. For zero forcing (ZF) case, the precoding matrix is given by $W^l = H^{lH}(H^l H^{lH})^{-1}$, where superscript H denotes the Hermite transpose operation.

This paper considers THP and VP as non-linear precoding case (Fig. 1(b)). For THP case, the estimated channel matrix is decomposed into $H^l = R^l Q^{lH}$, where $Q^l \in \mathbb{C}^{N_t \times MN_s}$ is the unitary matrix and $R^l \in \mathbb{C}^{MN_s \times MN_s}$ is the lower triangular

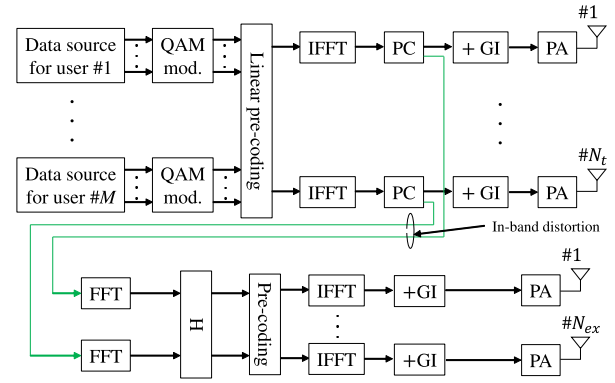

(a) Base station with linear pre-coding.

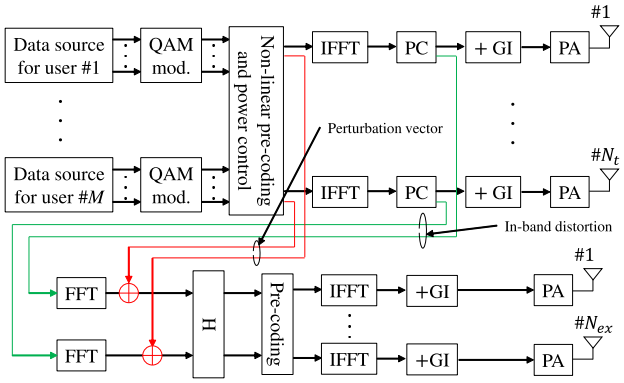

(b) Base station with non-linear pre-coding.

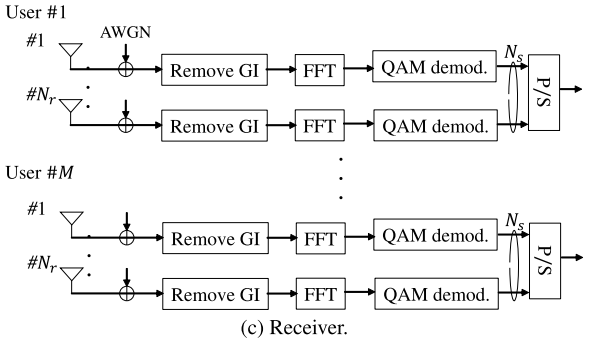

(c) Receiver.

FIGURE 1. mMIMO-OFDM system model.

matrix. Q^l is used as precoding weight. Based on the successive interference cancellation, the transmit symbol $\hat{s}_j^l$ is given as

$$\hat{s}_j^l = \bar{s}_j^l - \sum_{i=1}^{j-1} \bar{s}_i^l \frac{r_{ji}^l}{r_{jj}^l}, \tag{11}$$

where r_{ji}^l represents the (j, i) element of the matrix R^l. The perturbation vector p_j^l is used to limit $\hat{s}_j^l$ within a certain threshold τ, which is expressed as

$$\hat{s}_j'^l = \hat{s}_j^l + p_j^l, \tag{12}$$

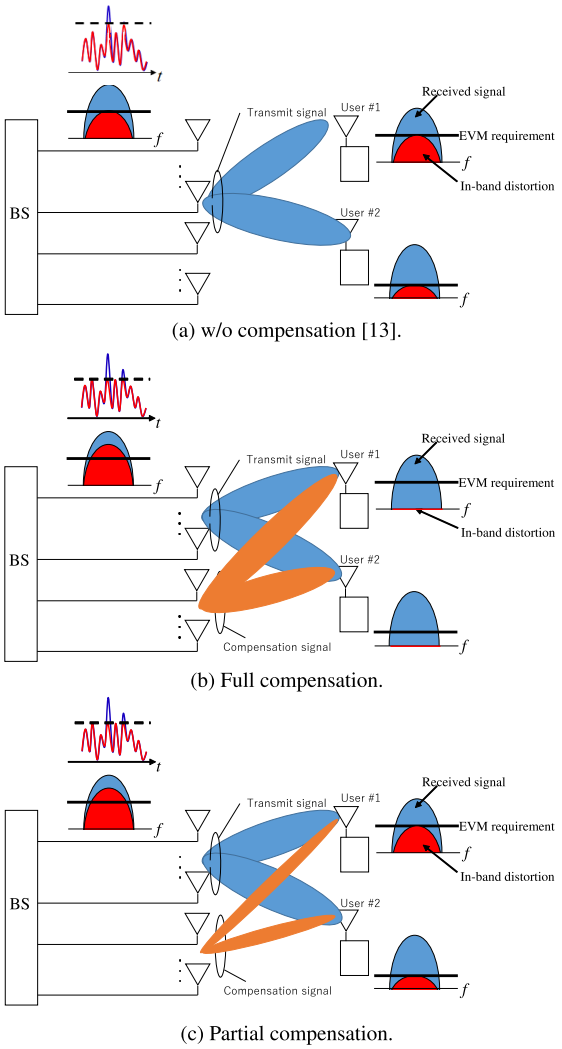

(a) w/o compensation [13].

(b) Full compensation.

(c) Partial compensation.

FIGURE 2. Illustration of the distortion compensation technique (M=2, N_r=1).

where p_j^l is given by using modulo operation. The precoded transmit signal vector is given as

$$x^l = P_t Q^l \hat{s}'^l, \tag{13}$$

where $\hat{s}'^l = [\hat{s}_1'^l, \hat{s}_2'^l, \ldots, \hat{s}_{MN_s}'^l]^T$. P_t is the normalization factor of the transmit power.

For VP case, transmission symbols are selected among the expanded constellation points to minimize the average power of the output signals at the precoder. The precoded transmit signal vector is given as $x^l = P_t W^l (s^l + p^l)$, where $p^l \in \mathbb{C}^{MN_s \times 1}$ is the perturbation vector. For QPSK modulation, p^l is independently selected for each subcarrier from 0, $\pm j\tau$, $\pm j(1+\tau)$, $\pm j(1-\tau)$. τ is the constellation interval.

III. PROPOSED METHOD

A. ENHANCED PEAK CANCELLATION WITH IN-BAND DISTORTION COMPENSATION

In this section, we propose an in-band distortion compensation method for enhancing adaptive peak cancellation (PC)

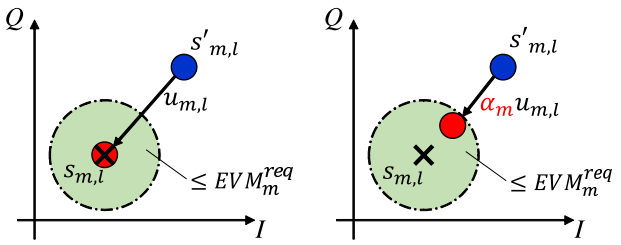

(a) Full compensation. (b) Partial compensation.

FIGURE 3. Signal constellation in case with adaptive in-band distortion compensation.

performance. In this method, the PC is applied at each antenna where the peak amplitude exceeding the peak detection threshold is repeatedly suppressed by adding the PC signal designed as a scaled OFDM symbol [12], [13]. Consequently, it causes in-band distortion that needs to be compensated. Here, the proposed method does not increase signal redundancy explicitly. Instead of that, the proposed method needs to use some extra antenna elements for in-band distortion compensation. Note that these extra antenna elements can be used for in-band distortion compensation or increasing precoding gain.

Figure 2 illustrates the concept of the distortion compensation using extra antennas for mMIMO-OFDM. Full compensation and Partial compensation are given in Figs. 2(a) and (b). In Fig. 2(c), peak cancellation without in-band compensation is adopted under EVM restriction, where in-band distortion is restricted below a permissible level. In this case, deep peak cancellation is not possible due to severe in-band distortion especially for higher order modulation such as 64QAM. On the other hand, unlike the above, in-band distortion cancellation signal is transmitted using extra antennas so that the receivers are never affected by the distortion (Fig. 2(b)). Furthermore, partial compensation (Fig. 2(b)) is used to minimize the required energy for the compensation, where in-band distortion is suppressed to a permissible level.

Figure 3 illustrates the constellation using the distortion compensation technique. In this figure, the cross mark is the original constellation point without any PAPR reduction. The blue and red circle represents the constellation points using adaptive PC with and without in-band distortion compensation technique, respectively. In the proposed technique shown in Fig. 3(b), unlike the full-compensation technique in Fig. 3(a), the constellation point is compensated to the green shaded area that it meets the EVM requirement.

Let $x^l \in \mathbb{C}^{N_t \times 1}$ and $\tilde{x}^l \in \mathbb{C}^{N_t \times 1}$ denote the transmit signal vector expression of l-th subcarrier before and after peak cancellation, respectively. The relationship between $x^l$and $\tilde{x}^l$ is given as

$$\tilde{x}^l = x^l + d^l, \tag{14}$$

where $d^l \in \mathbb{C}^{N_t \times 1}$ is an in-band distortion at l-th subcarrier. In other words, an in-band distortion component is given as

$$d^l = \tilde{x}^l - x^l. \tag{15}$$

The received signal vector is given as

$$\begin{aligned} y^l &= H^l \tilde{x}^l + n^l \\ &= H^l (x^l + d^l) + n^l \\ &= P_t H^l (W^l s^l + d^l) + n^l \\ &= \underbrace{P_t s^l}_{\text{desired signal}} + \underbrace{P_t H^l d^l}_{\text{in-band distortion}} + \underbrace{n^l}_{\text{noise}}, \end{aligned} \tag{16}$$

where first, second, and third terms denote desired signal, noise and in-band distortion at the user side. To cancel the in-band distortion, the base station transmits the distortion compensation signal through the extra antenna. In the following sentence, we explain how to generate the distortion compensation signal. First, base station estimates the received distortion signal $u^l = [u_{1l}, u_{2l}, \ldots, u_{MN_s l}]^T \in \mathbb{C}^{MN_s \times 1}$ as

$$u^l = \hat{H}^l d^l, \tag{17}$$

where $\hat{H}^l \in \mathbb{C}^{MN_s \times N_t}$ is the estimated channel matrix. Then, EVM of each stream when adaptive PC is applied can be estimated by using Eq. (17) as below.

$$\xi_j^{est} = \sum_{l=0}^{L-1} |u_{jl}|^2 / \sum_{l=0}^{L-1} |\bar{s}_{jl}|^2. \tag{18}$$

The estimated received signal vector u^l is precoded as

$$z^l = -\bar{W}^l u^l, \tag{19}$$

where z^l is the distortion compensation signal transmitted using extra antennas. $\bar{W}^l \in \mathbb{C}^{N_{ex} \times MN_s}$ denotes the ZF precoding weight for the channel $\bar{H}^l \in \mathbb{C}^{MN_s \times N_{ex}}$ between extra antennas and users. The received signal vector with distortion compensation is given as

$$\begin{aligned} y^l &= H^l \tilde{x}^l + \bar{H}^l z^l + n^l \\ &= H^l (x^l + d^l) - u^l + n^l \\ &= P_t s^l + (H^l - \hat{H}^l) d^l + n^l \\ &= P_t s^l + \Delta H^l d^l + n^l, \end{aligned} \tag{20}$$

where ΔH^l denotes the channel estimation error. From the above equations, in-band distortion is perfectly removed if perfect channel estimation is assumed ($\Delta H^l = 0$).

B. OPTIMIZATION OF IN-BAND DISTORTION COMPENSATION UNDER EVM RESTRICTION

To control achieved EVM stream-by-stream, we define distortion control factor as an diagonal matrix:

$$A = diag(\alpha_1, \alpha_2, \ldots, \alpha_j, \ldots, \alpha_{MN_s}) \in \mathbb{R}^{MN_s \times MN_s}. \tag{21}$$

where α_j denotes a factor to control EVM value of the j-th stream ($0 \leq \alpha_j \leq 1$), i.e., $\alpha_j = 1$ corresponds to full compensation while $\alpha_j = 0$ corresponds to no compensation.

Eq. (17) is multiplied by A to reduce the transmit power of the distortion compensation signal as

$$u^{'l} = Au^l. \tag{22}$$

Eq. (22) is precoded by Eq. (19) and transmitted from extra antennas as

$$z^{'l} = -W^l u^{l'}. \tag{23}$$

The received signal of j-th stream using is given as

$$\begin{aligned} y'_{jl} &= \sum_{n=1}^{N} H^l_{jn}\tilde{x}^l_n + \sum_{k=1}^{N_{ex}} \bar{H}^l_{jk} z^{'l}_k + n^l_j \\ &= \sum_{n=1}^{N} H^l_{jn}(x^l_n + d^l_n) - \alpha_j \sum_{n=1}^{N} H^l_{jn} d^l_l + n^l_j \\ &= P_t s^l_j + (1-\alpha_j) r^l_j + n^l_j, \end{aligned} \tag{24}$$

where H_{ij} and $\bar{H}_{ij}$ are (i,j)-th element of matrix H^l and $\bar{H}^l$, respectively. $x^l_i, \tilde{x}^l_i, d^l_i$ and $z^{'l}_i$ are i-th element of vector $x^l, \tilde{x}^l$, d^l, and $z^{'l}$, respectively. The achieved EVM is given as

$$\begin{aligned} \xi_j &= \sum_{l=-L/2}^{L/2+1} |(1-\alpha_j)u_{jl}|^2 / \sum_{l=-L/2}^{L/2+1} |s_{jl}|^2 \\ &= (1-\alpha_j)^2 \sum_{l=-L/2}^{L/2+1} |u_{jl}|^2 / \sum_{l=-L/2}^{L/2+1} |s_{jl}|^2 \\ &= (1-\alpha_j)^2 \xi^{est}_m. \end{aligned} \tag{25}$$

The optimum α_j to meet EVM constraint is given as follows.

$$\alpha_j = \begin{cases} \left(1 - \sqrt{\dfrac{\xi^{req}_m}{\xi^{est}_m}}\right) & (\xi^{req}_j < \xi^{est}_j) \\ 0 & (\text{otherwise}), \end{cases} \tag{26}$$

where if the target EVM value for m-th user satisfies the requirement ($\xi_j < \xi^{req}_j$), $\alpha_j = 0$ is used. Then, average received SDNR (Signal to distortion and noise ratio) is defined as

$$SDNR = \frac{E[||H_l \tilde{x}_l||_2^2]}{E[||(I_{MN_s \times MN_s} - A)U_l||_2^2] + E[n_l||_2^2]}, \tag{27}$$

where $||\cdot||_2^2$ denotes the Euclidian norm. $E[\cdot]$ is the ensemble average operation and $I_{MN_s \times MN_s}$ is the identity matrix.

C. ENHANCED PEAK CANCELLATION FOR NON-LINEAR PRECODED mMIMO-OFDM SYSTEMS

We improve the proposed method for non-linear precoded mMIMO-OFDM system with peak cancellation. Here, the perturbation vector of power control is superimposed on the in-band distortion compensation signal for PC. This method does not need the modulo operation at the receiver side, and thus modulo error never occur unlike the conventional non-linear precoded systems.

In THP, the received signal vector vector in case with enhanced peak cancellation is given as

$$\begin{aligned} y^l &= H^l \tilde{x}^l + n^l \\ &= H^l x^l + H^l d^l + n^l \\ &= R^l (P_t Q^l (\hat{s}^l + p^l) + H^l d^l) + n^l \\ &= \underbrace{P_t diag(R_{mm}) s^l}_{\text{desired signal}} + \underbrace{P_t diag(R_{mm}) p^l}_{\text{perturbation vector}} \\ &\quad + \underbrace{R^l H^l d^l}_{\text{in-band distortion}} + \underbrace{n^l}_{\text{noise}}, \end{aligned} \tag{28}$$

where $diag(R_{mm})$ is a diagonal matrix with $r_{11}, r_{22}, \ldots, r_{MN_sMN_s}$, $p^l = [p^l_1, p^l_2, \ldots, p_{MN_s}]^T$ and $\tilde{x}^l$ is the transmit vector after applying adaptive PC. In the proposed method, the received perturbation vector is superimposed on the distortion compensation signal in Eq. (17).

$$\hat{u}^l = -(R^l H^l d^l + P_t diag(R_{jj}) p^l). \tag{29}$$

$\hat{u}^l$ is precoded with ZF precoder according to the Eq. (19) and transmitted from extra antennas. The received signal expression of the TH precoded mMIMO-OFDM using proposed method is given as

$$\begin{aligned} y^l &= H^l \tilde{x}^l + \bar{H}^l \bar{W}^l \hat{u}^l + n^l \\ &= R^l (x^l + H^l d^l) - (R^l H^l d^l + P_t diag(R_{jj}) p^l) + n^l \\ &= P_t diag(R_{mm}) s^l + n^l. \end{aligned} \tag{30}$$

However, a perturbation vector based on a modulo operation has high power and it may cause an increase of the compensation signal. In the proposed method, the perturbation vector should be as short as possible to suppress the required energy for compensation, i.e., keep the precoding gain for data transmission. Therefore, we apply the simple power control to the real and imaginary parts of each subcarrier instead of the modulo operation.

$$F_\tau(x) = \begin{cases} \tau \dfrac{x}{|x|} & x > \tau \\ x & (\text{otherwise}). \end{cases} \tag{31}$$

The concept of the proposed power control is illustrated in Fig.4. As in this figure, the perturbation vector length can be minimized in the proposed approach unlike traditional modulo operation. The transmit vector after applying the power control in Eq. (31) is given as

$$\hat{s}^{''l}_j = F_\tau(Re[\hat{s}^l_j]) + jF_\tau(Im[\hat{s}^l_j]), \tag{32}$$

where perturbation vector is given as

$$p^l_j = \hat{s}^{''l}_j - \hat{s}^l_j. \tag{33}$$

The perturbation vector in Eq. (33) is superimposed to the distortion compensation signal as in Eq. (29), and transmitted by extra antennas.

In VP, the computational complexity is increased to find the optimum perturbation vector. Therefore, the complexity reduction is a challenging problem. In the proposed method,

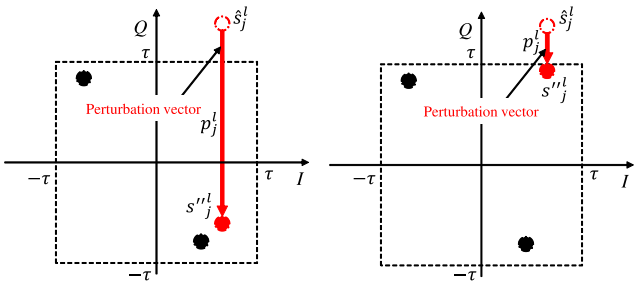

(a) Traditional modulo. (b) Proposed.

FIGURE 4. The concept of the proposed power control method for TH precoded mMIMO-OFDM systems.

similarly to case with THP, the perturbation vector of the power control at the base station is superimposed on the in-band distortion compensation signals. This means that modulo operation is not required on the receiver side. Furthermore, in the proposed method, subcarrier-wise power control can be applied directly to the output signals of the precoder, and thus there is no need to optimize the perturbation vector. We apply the simple power control to the precoded transmit signal similarly to the THP case in Eq.(31). The output signal after the power control is given by

$$x_n^{'l} = F_\tau(Re[x_n^l]) + jF_\tau(Im[x_n^l]). \tag{34}$$

It is clear that the proposed power control approach is able to reduce the required computational complexity for searching the optimum perturbation vector. Let $x^{'l} = [x_1^{'l}, x_2^{'l}, \ldots, x_N^{'l}]^T$ denote the transmit signal vector after the power control. The received perturbation vector is defined as $p^l = H^l(x^{'l} - x^l)$. Hence, the distortion compensation signal in VP is given as

$$\hat{u}^{'l} = \hat{H}^l d^l + p^{'l}. \tag{35}$$

The received signal expression is follows.

$$\begin{aligned} y^{'l} &= H^l(x^{'l} + d^l) + \bar{H}^l \bar{W}^l \hat{u}^{'l} + n^l \\ &= P_t s^l + H^l d^l + p^l - (H^l d^l + p^{'l}) + n^l \\ &= P_t s^l + n^l, \end{aligned} \tag{36}$$

where we assume the perfect channel estimation.

IV. RELATED WORKS

Several PAPR reduction techniques for mMIMO-OFDM signals have been proposed in the literature [14]–[25]. One of the typical approaches is to solve the optimization problem that minimizes the PAPR under the restriction of inter-user interference (IUI) [14]–[16]. In [14], an iterative PAPR reduction method based on a fast iterative shrinkage thresholding algorithm (FITRA) is proposed, where a limiter-based PAPR reduction and its in-band distortion compensation are repeated until it converges. This method achieves both PAPR reduction and in-band distortion compensation in an iterative manner. However, high computational complexity is required for iterative processing to obtain converged performance. In [15], a generalized approximate message passing (GAMP) algorithm based PAPR reduction method is utilized to solve the above problem. Since each iteration requires simple matrix and vector multiplications, this method achieves lower computational complexity and higher convergence than those in [14] while achieving lower PAPR. However, since the IUI cannot be completely removed, BER is degraded due to residual IUI. In [16], an in-band distortion compensation technique due to peak limiter is proposed, where extra streams are added to compensate for the in-band distortion. This method utilizes a part of data streams to restrict PAPR without distorting data streams, i.e., available streams are divided into "for data transmission" and "for in-band distortion compensation", where data are preferentially transmitted on high gain streams while the remaining streams are used for in-band distortion compensation. This method can achieve a lower complexity than FITRA based methods. However, iterative processing is still needed which results in increased computational complexity. In [17], an in-band distortion compensation technique utilizing extra antennas are proposed for a limiter based PAPR reduction. In this method, extra antennas at the base station are used to perform in-band distortion compensation, where the number of the extra antenna is properly selected. Unlike the works in [14]–[16], this method does not require any iterative processing for in-band distortion compensation. However, work in [17] does not consider the peak regrowth due to filtering to remove OoB radiation and thus to reduce signal amplitude below a given threshold, iterative processing such as iterative clipping & filtering is needed. In addition, this work does not consider the non-linear precoding case. In [18], [19], the authors proposed to use constant envelope modulation for data transmission in mMIMO. In this method, the phase of the transmit signal is optimized to minimize the multi-user interference, where the amplitude of the transmit signal is constant. However, the possible application of this method is limited. In addition, residual IUI remains on the user side which may degrade BER. In [20], an adaptive tone reservation (TR) based PAPR reduction scheme for mMIMO is proposed as a distortion-less approach, where TR is iteratively carried out if per-antenna peak power exceeds a given threshold. However, this method uses a part of subcarriers for PAPR reduction and thus data rate decreases as the number of reserved tones increases. In [21], a PAPR reduction method using the perturbation vector is proposed. In this method, a perturbation vector is designed to reduce the PAPR by using the dimension of the null space and thus distortion-free PAPR suppression can be achieved. Since this method is carried out independently from precoding design, it does not require re-calculating precoding matrix iteratively for PAPR reduction and thus any precoders are applicable. However, the computational cost is increased to optimize the perturbation vector to sufficiently reduce the PAPR. In [22], [23], a complexity-reduced peak cancellation based PAPR reduction technique and its in-band distortion compensation by utilizing null space is proposed for MIMO systems. In this method, a peak cancellation signal is projected onto the null space of the mMIMO-channel to avoid

in-band distortion compensation and consequently achieve better throughput performance. However, achieved peak cancellation may depend on precoding design. In addition, an extension to non-linear precoding is not presented. In [24], a two-dimensional tone reservation method utilizing reserved tones and unused beams are proposed where peak cancellation signals are designed by combining the frequency-domain PAPR reduction (i.e., TR) and space-domain PAPR reduction (i.e., utilizing the unused beam). However, this method requires extra subcarriers, in addition, extra beams (i.e., spatial degree of freedom). In addition, required computational complexity is increased to generate two-dimensionally optimized tones for PAPR reduction. In [25], a vector perturbation based non-linear precoding method with PAPR reduction is proposed where a perturbation vector is designed to minimize both the average power and PAPR of the transmit signal. However, in this work, the same or higher complexity than the conventional VP may be needed to search the optimum perturbation vector.

Unlike the previous related works, this paper presents an enhanced peak cancellation framework with a low complexity in-band distortion compensation for mMIMO-OFDM, which is applicable to both linear and non-linear precoding.

V. PERFORMANCE EVALUATION AND DISCUSSIONS

The number of antennas at the base station is $N_t + N_{ex}$ and the number of users is M. N_{ex} denotes the number of extra antennas used for in-band distortion compensation. The number of subcarriers is 64. Six-path Rayleigh fading is assumed as each path model of mMIMO channel. In the peak cancellation, adjacent channel leakage power ratio (ACLR) is kept below the required value (−50dB) [13]. In this paper, we have evaluated the impact of increasing extra antenna elements under the condition where the number of total transmit antennas and the total transmission power are the same.

Solid state power amplifier (SSPA) model [27] is used for nonlinear power amplifiers. The input/output characteristic of the SSPA is given by

$$|y(t)| = \frac{\beta |x(t)|}{(1 + (|x(t)|/\sqrt{P_s})^{2p})^{\frac{1}{2p}}}, \tag{37}$$

where $x(t)$ and $y(t)$ are input and output signals of the SSPA. p is a non-linear factor and β is a gain. P_s is the saturation output power. In the SSPA, input back off (IBO) is defined as the average input signal power P_a normalized by a saturation output power, $IBO = 10log_{10}(P_a/P_s)$.

For comparison, we evaluate the performance of a limiter based iterative PAPR reduction and its in-band distortion compensation method, MU-PP-GDm, in [16]. In the MU-PP-GDm, limiter based PAPR reduction is carried out and its in-band distortion is compensated by using streams transmitted through lower gain spatial channel. Here, the precoding matrix to remove the inter-user interference is calculated using an iterative gradient descent approach. We also compare the proposed method with the PC with an iterative in-band distortion compensation method in Fig. 5. In this

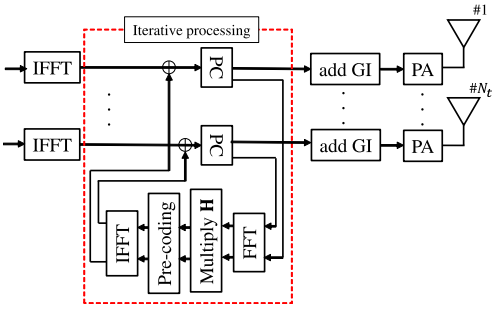

FIGURE 5. Block diagram of the iterative in-band distortion compensation method for mMIMO-OFDM systems with adaptive PC.

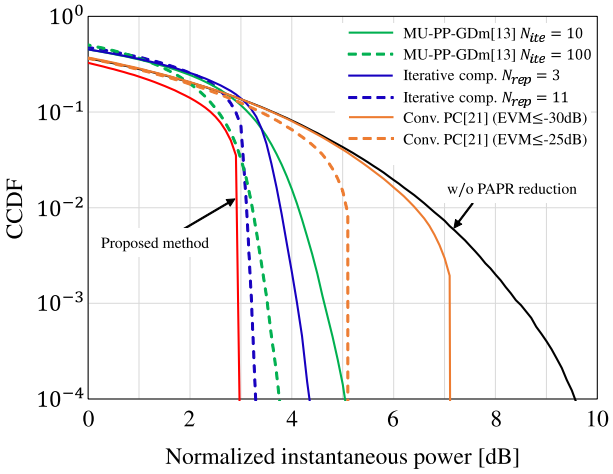

FIGURE 6. CCDF characteristics of the normalized instantaneous power of the linear-precoded mMIMO-OFDM signals.

method, PC and in-band distortion compensation are repeated alternately until the peak amplitude is suppressed below the threshold level. If the number of antennas is large enough (i.e., $N_t > MN_s$), this method is applicable.

A. PAPR

To clarify the effectiveness of the proposed method, we evaluate the CCDFs of the normalized instantaneous power of the transmit signals. CCDF is defined as the probability that the random variable Z exceeds z,

$$CCDF(z) = Prob(Z \geq z) = \int_z^{\infty} P(t)dt, \tag{38}$$

where $P(t)$ denotes the PDF of the random variable t.

Figure 6 shows the CCDF of the normalized instantaneous power of the transmit signal per an antenna, where instantaneous power is normalized by the average power of the transmit signal before PAPR reduction. In Fig. 6, the green lines show the performance of the MU-PP-GDm in [16], where peak detection threshold is set to 3dB and the number of iteration for the MU-PP-GDm algorithm N_{ite} is set to 10 and 100. The blue lines show the performance of the adaptive PC with iterative in-band distortion compensation

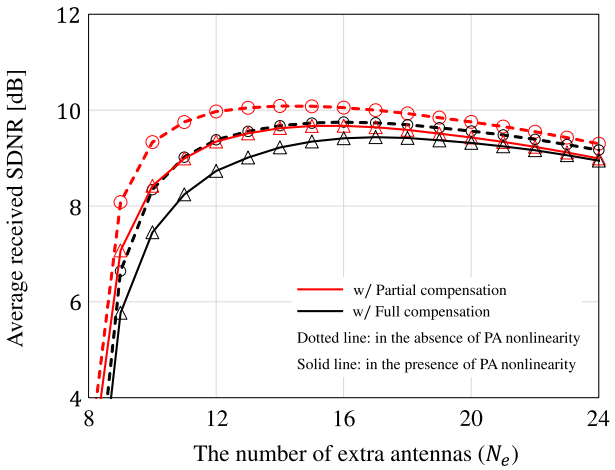

FIGURE 7. SDNR performances of the ZF precoded mMIMO-OFDM systems.

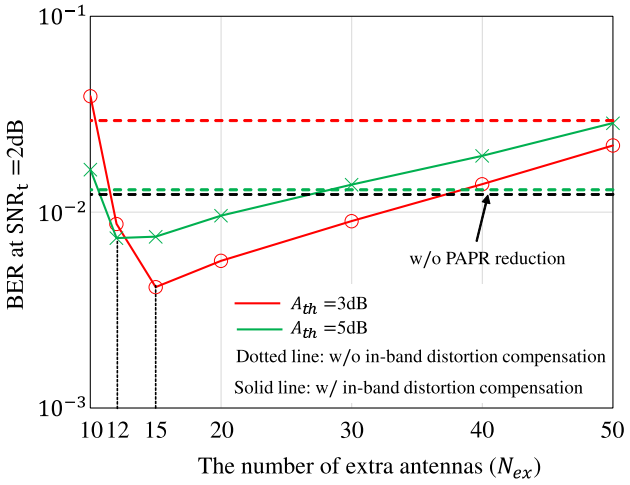

FIGURE 8. The relation between the number of extra antennas and BER of the ZF precoded mMIMO-OFDM systems.

technique in FIg. 5, where the number of iteration for this method N_{ite} is set to 3 and 11. The red line shows the performance of the proposed method using adaptive PC with in-band distortion compensation utilizing extra antennas, where the number of extra antennas is set to $N_{ex} = 20$. In these methods, the peak detection threshold is set to 3dB. The orange lines show the performance of the adaptive PC without any in-band distortion compensation (i.e., conventional adaptive PC [12], [13], where EVM of the transmit signals is kept under required value. We assume the EVM ≤ -25dB for 16QAM and EVM ≤ -30dB for 64QAM signals, respectively. From Fig. 6, achieved PAPR of the proposed method is much lower than the conventional PC [12], [13]. This is because the conventional adaptive PC suffers from severe EVM constraints especially for higher-order QAM, unlike the proposed method can compensate in-band distortion and consequently achieve target PAPR value regardless of the modulation order. We also confirm that the proposed method achieves lower PAPR than cases with the iterative in-band distortion compensation and the MU-PP-GDm in [16], because both the conventional methods need more iterations to obtain converged performance. Unlike these conventional methods, the proposed in-band distortion compensation method is not iterative manner and thus it is clear that PAPR can be minimized with much lower complexity than the others.

B. SDNR

Figure 7 shows the received SDNR defined in Eq.(27) in the ZF precoded mMIMO-OFDM with adaptive PC and its in-band distortion compensation utilizing extra antenna set. The number of total antennas at the base station is set to $N_t + N_{ex} = 64$. The number of users and the number of received antennas are set to $M = 8$ and $N_r = 1$, respectively, where 4 users use QPSK and the other 4 users use 64QAM. Transmit SNR per antenna is set to -5dB. In peak cancellation, peak detection threshold is set to 3dB while the required EVM is -20dB for QPSK and -30dB for 64QAM, respectively. In this figure, solid lines and dotted lines show the SDNR in the presence of PA nonlinearity (IBO=3dB) and in the absence of PA nonlinearity, respectively. For comparison, we also evaluate SDNR for the full compensation (black line) and the partial compensation (red line). In the partial compensation, the in-band distortion is partially compensated to a permissible level user-by-user. From this figure, we can confirm that the adaptive (partial) compensation method can achieve higher received SDNR compared to the full compensation case. We can also see that SDNR can be maximized at $N_{ex} = 14$ for the partial compensation at and $N_{ex} = 17$ for the full compensation case in the presence of PA nonlinearity. This means that the required number of extra antennas can be minimized by avoiding full compensation which results in increasing the precoding gain.

C. BER

In this paper, we define the transmit SNR as SNR per transmit antenna when channel gain is normalized which is given as

$$SNR_t = \frac{E[|x^l|_2^2]}{E[|n^l|_2^2]} = \frac{P_t E[|W^l s^l|_2^2]}{E[|n^l|_2^2]} \tag{39}$$

where x^l and n^l denote transmit signal vector and noise vector expressions of l-th subcarrier, respectively. s^l and W^l are transmit data vector and precoding weight matrix of l-th subcarrier, respectively. Figure 8 represents the relation between achieved BER and the number of extra antennas N_{ex} in mMIMO-OFDM systems with ZF precoding, where $N_t + N_{ex} = 100$, $M = 10$ and $N_r = 1$, respectively. 64QAM is used. IBO of SSPA is set to 4dB. In Fig. 8, solid lines and dotted lines show the case with and without in-band distortion compensation technique, respectively. In the case without in-band distortion, all transmit antennas are used for data transmission. The black line represents the case where PAPR reduction is not applied. In this case, high peak amplitudes of the transmit signal cause the nonlinear

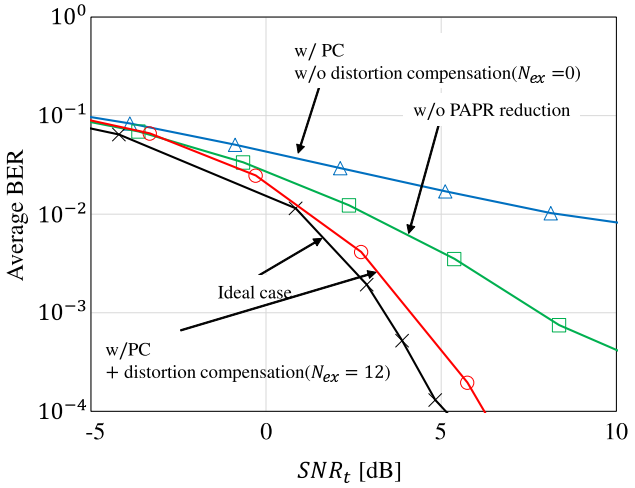

FIGURE 9. BER performance of the ZF precoded mMIMO-OFDM systems.

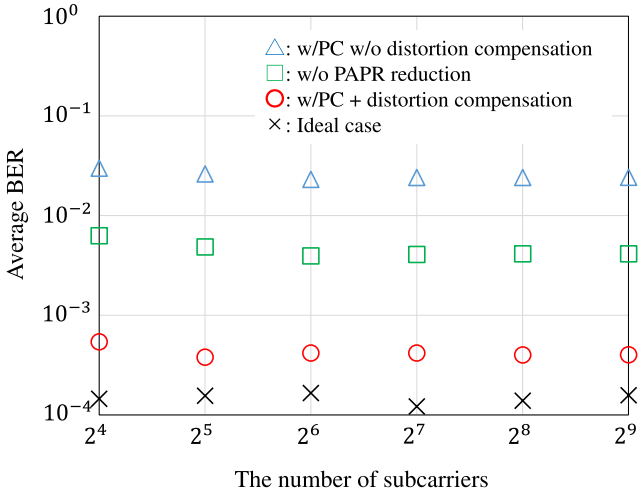

FIGURE 10. The relation between the number of subcarriers and BER.

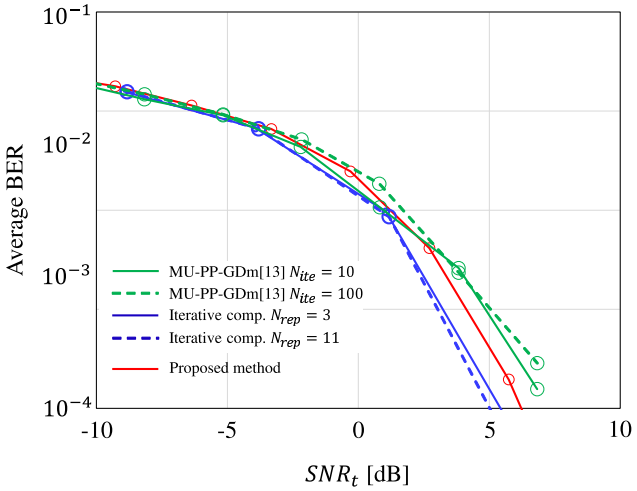

FIGURE 11. BER comparison between the proposed method and conventional method.

distortion at the transmit PA and it results in BER degradation. The red and green lines show the BER performance of the proposed method with A_{th}^2 =3dB and 5dB, respectively. From this figure, it can be confirmed that BER increases as N_{ex} increases when $N_{ex} > 15$ for $A_{th}^2 = 3$dB and $N_{ex} > 12$ for $A_{th}^2 = 5$dB, respectively. This is because the antenna gain decreases as N_{ex} increases when the total number of the transmit antennas $(N_t + N_{ex})$ is constant. On the other hand, when N_{ex} is small, BER increases because the transmission power of the distortion compensation signals increase and it causes the nonlinear distortion at the PA of the extra antennas. From Fig. 8, we can confirm that BER can be minimized when $N_{ex} = 12$ for $A_{th}^2 = 5$dB and $N_{ex} = 15$ for $A_{th}^2 = 3$dB, respectively.

Figure 9 shows BER performance of the ZF precoded mMIMO-OFDM systems using adaptive PC and in-band distortion compensation, where $N_t = 88$ and $N_{ex} = 12$. Spatial correlation factors are set to $\beta_r = 0$ and $\beta_t = 0$. IBO of the SSPA is set to 4dB. The peak detection threshold is set to $A_{th}^2 = 3$dB. The red line shows BER of mMIMO-OFDM with the proposed method where the number of extra antennas is set to $N_{ex} = 12$. For comparison, we evaluate the ideal case depicted by black line where any non-linear distortion does not occur at the transmit PA and in-band distortion is compensated without any penalty. In addition, the green line shows BER of the case without PAPR reduction while the blue lines corresponds to case of the adaptive PC without in-band distortion compensation. From this figure, we can see that the proposed method can improve BER performance significantly compared with the other methods suffering from non-linear distortion at PA and in-band distortion due to peak cancellation.

According to the definition of SDNR in Eq.(27), it is clear that the same BER performance can be obtained by the proposed method for a different number of subcarriers as far as SDNR is the same. Figure 10 s hows the relation between achieved BER and the number of subcarriers for the case with the proposed method, where SNR is 5dB and PAPR =3dB at CCDF=10^{-4} is achieved by peak cancellation. It can be confirmed from this result that almost the same BER is achieved for cases with a various number of subcarriers.

Figure 11 shows the BER comparison of mMIMO-OFDM with the proposed method, the MU-PP-GDm [16], and iterative in-band distortion compensation, where 64QAM is used at each subcarrier. IBO of the SSPA is set to 4dB. The proposed method with full-compensation is used where $N_{ex} = 12$ and $A_{th}^2 = 3$dB. For comparison, the ideal case is also shown. The solid and dotted green lines show cases of MU-PP-GDm with $N_{ite} = 10$ and 100, respectively. From this figure, we can confirm that the proposed method achieves better BER than that of MU-PP-GDm which suffers from residual inter-user interference. Although BER of the iterative compensation method is slightly better than the proposed one, it is worth mentioning that the proposed method achieves

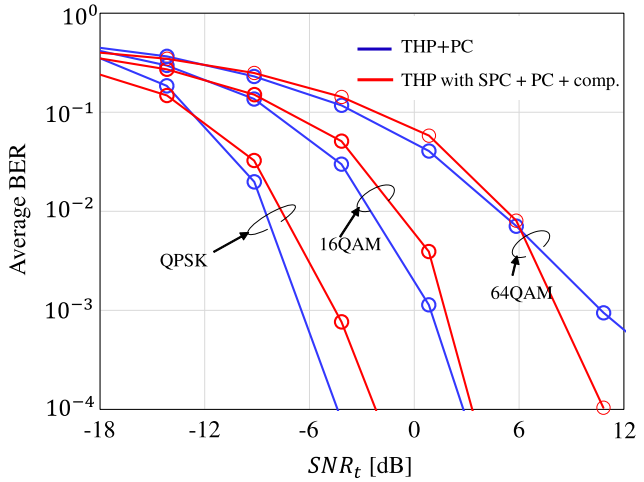

(a) with THP.

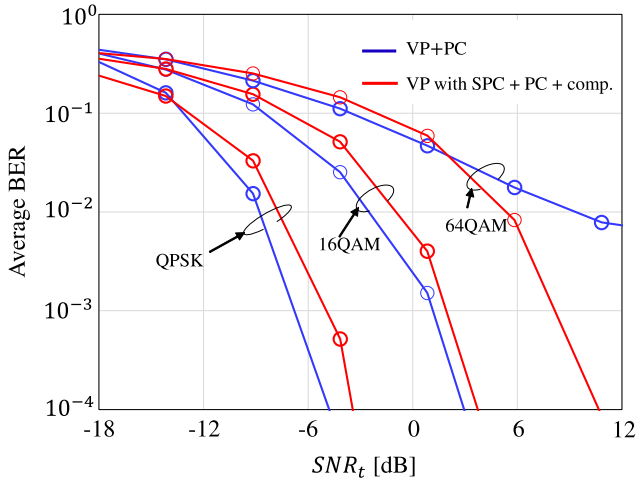

(b) with VP.

FIGURE 12. BER performance of non-linear precoded mMIMO-OFDM with the proposed method.

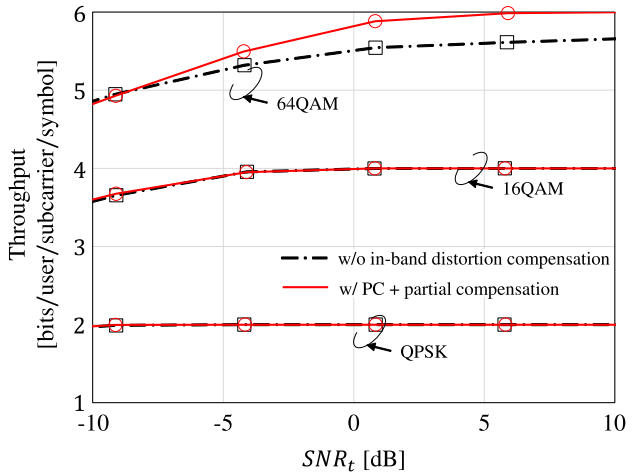

(a) Spatial multiplexing with the same modulation.

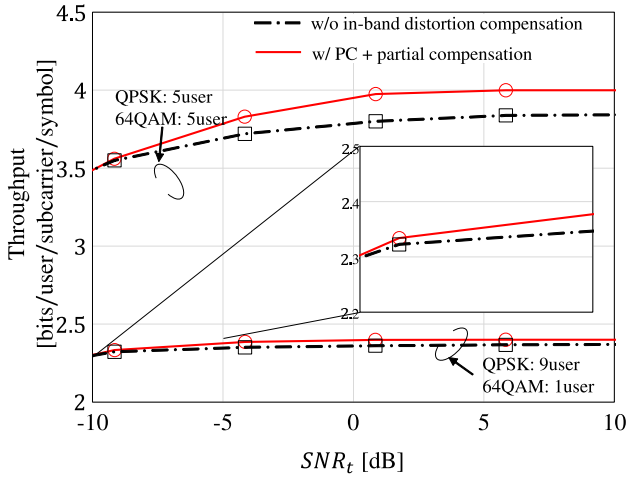

(b) Spatial multiplexing with different modulation.

FIGURE 13. Throughput performance of mMIMO-OFDM with the proposed method, where ZF precoding is used.

lower PAPR than this method in the same condition with much lower complexity (i.e., without iterative compensation) as in Fig. 6.

Figure 12 shows BER performance of mMIMO-OFDM systems with nonlinear precoding (THP and VP). Here, we assume $N_t = 50$, $N_{ex} = 30$, $M = 4$, $N_r = 4$, and $\beta_t = \beta_r = 0.5$. 64QAM is used. IBO of SSPA is set to 6dB. A_{th}^2 is set to 5dB. In these figures, the label "THP (VP) + PC" is BER performance of the conventional THP (VP) with adaptive PC [12], where in-band distortion compensation is not applied and it is kept below a permissible value. The label "THP (VP) with SPC+PC+comp.," is BER performance of the THP (VP) with subcarrier power control (SPC) in Eq.(31), where the perturbation vector is superimposed on the in-band distortion compensation signal. In the PC [12], required EVM is set to −20dB for QPSK, −25dB for 16QAM, −30dB for 64QAM, respectively. From these figures, in QPSK case, "THP (VP) with SPC + PC + comp." shows better BER performance than "the THP with PC" because modulo error never occurs in the proposed method. It is also confirmed that in 64QAM case, "THP (VP) with SPC + PC + comp." shows the best BER in higher SNR region because of in-band distortion compensation effect. For high-order modulation case, in-band distortion compensation is necessary.

D. THROUGHPUT

In this section, we evaluate the achievable throughput performance of the proposed method. Throughput is defined as the number of correctly received data bits per stream, per subcarrier, per symbol.

$$Throughput = \frac{N_b^{tot}}{M \times N_r \times N_{symbol}}, \tag{40}$$

where N_b^{tot} denotes the number of total transmitted bits and the number of received bits without error. N_{symbol} is the number of received symbols. In this section, the number of

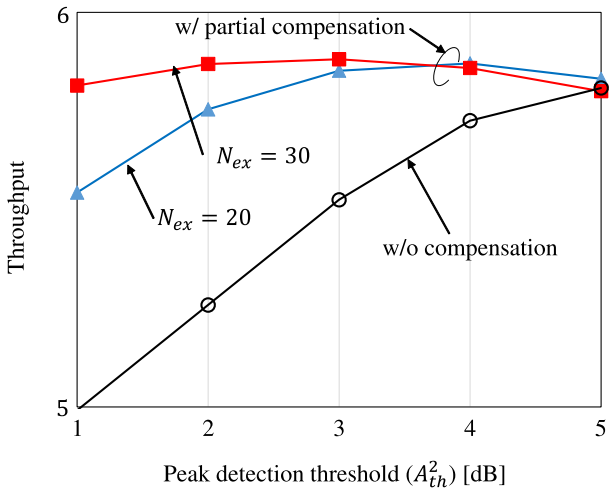

FIGURE 14. Relation between peak detection threshold A_{th}^2 and throughput in mMIMO-OFDM with the proposed method, where ZF precoding is used.

transmit antennas and the number of extra antennas at the base station are set to $N_t = 80$ and $N_{ex} = 20$, respectively.

Figure 13 shows the relation between transmit SNR (SNR_t) and throughput, where each user uses same modulation type. In Fig. 13, the black lines show the case without in-band distortion compensation, where $N_t = 100$ and adaptive PC with $A_{th}^2 = 3$dB is used. The red line shows the case with in-band distortion compensation. From this figure, when the modulation order is low, in-band distortion compensation is not effective for improving the throughput performance. If the modulation order increases, the proposed method works more effectively because degradation due to in-band distortion becomes severe in high-order modulation.

Figure 13(b) shows the relation between transmit SNR (SNR_t) and throughput. The number of users and the number of received antennas are set to $M = 10$ and $N_r = 1$, respectively. In this figure, the black lines show the case without in-band distortion compensation, where $N_t = 100$ and adaptive PC with $A_{th}^2 = 3$dB is used. The red line shows the case with the partial (adaptive) compensation. From this figure, it can be seen that the throughput can be improved when in-band distortion compensation is used.

Figure 14 shows the relation between peak detection threshold A_{th}^2 and throughput, where $N_t + N_{ex} = 100$ is kept constant. Simulation parameters are the same as those of Fig. 13. The bule and the red lines show the case with partial compensation. 64QAM is used as subcarrier modulation. This figure show that peak cancellation with in-band distortion compensation achieves higher throughput than case without the compensation especially in lower peak detection threshold region. In addition, we can also see that in-band distortion compensation performance is improved by increasing the number of extra antennas N_{ex} in lower threshold region while higher throughput is obtained if N_{ex} is smaller number in higher threshold region. This is because precoding gain is decreased as N_{ex} increases. It is clear that the throughput can be maximized at $A_{th}^2 = 3$dB for $N_{ex} = 30$.

VI. CONCLUSION

This paper presented an enhanced peak cancellation framework with simplified in-band distortion compensation utilizing extra degree of freedom in mMIMO-OFDM systems. Unlike conventional methods, our proposed method achieves in-band distortion compensation without any additional processing at the receiver. In addition, the required degree of freedom for compensating in-band distortion due to peak cancellation can be minimized by choosing proper target EVM values for each user. Simulation results verify the effectiveness of the proposed method in terms of CCDF, SDNR, BER, and throughput. Performance analysis of the proposed mMIMO system with interference coordination is one of our future works.

REFERENCES

[1] T. L. Marzetta, "Noncooperative cellular wireless with unlimited numbers of base station antennas," *IEEE Trans. Wireless Commun.*, vol. 9, no. 11, pp. 3590–3600, Nov. 2010.
[2] H. Q. Ngo, *Massive MIMO: Fundamentals and System Designs*, vol. 1642. Linköping, Sweden: Linköping Univ. Electronic Press, 2015.
[3] Y. Rahmatallah and S. Mohan, "Peak-to-average power ratio reduction in OFDM systems: A survey and taxonomy," *IEEE Commun. Surveys Tuts.*, vol. 15, no. 4, pp. 1567–1592, Mar. 2013.
[4] R. W. Baüml, R. F. H. Fischer, and J. B. Huber, "Reducing the peak-to-average power ratio of multicarrier modulation by selected mapping," *Electron. Lett.*, vol. 32, no. 22, p. 2056, 1996.
[5] D.-W. Lim, J.-S. No, C.-W. Lim, and H. Chung, "A new SLM OFDM scheme with low complexity for PAPR reduction," *IEEE Signal Process. Lett.*, vol. 12, no. 2, pp. 93–96, Feb. 2005.
[6] H.-Y. Liang, "Selective mapping technique based on an adaptive phase-generation mechanism to reduce peak-to-average power ratio in orthogonal frequency division multiplexing systems," *IEEE Access*, vol. 7, pp. 96712–96718, 2019.
[7] S. H. Müller and J. B. Huber, "OFDM with reduced peak-to-average power ratio by optimum combination of partial transmit sequences," *Electron. Lett.*, vol. 33, no. 5, pp. 368–369, Feb. 1997.
[8] L. J. Cimini and N. R. Sollenberger, "Peak-to-average power ratio reduction of an OFDM signal using partial transmit sequence," *IEEE Commun. Lett.*, vol. 4, no. 3, pp. 86–88, Mar. 2000.
[9] Z. Zhou, L. Wang, and C. Hu, "Low-complexity PTS scheme for improving PAPR performance of OFDM systems," *IEEE Access*, vol. 7, pp. 131986–131994, 2019.
[10] I. Sohn and S. C. Kim, "Neural network based simplified clipping and filtering technique for PAPR reduction of OFDM signals," *IEEE Commun. Lett.*, vol. 19, no. 8, pp. 1438–1441, Aug. 2015.
[11] K. Anoh, C. Tanriover, B. Adebisi, and M. Hammoudeh, "A new approach to iterative clipping and filtering PAPR reduction scheme for OFDM systems," *IEEE Access*, vol. 6, pp. 17533–17544, 2018.
[12] T. Kageyama, O. Muta, and H. Gacanin, "An adaptive peak cancellation method for linear-precoded MIMO-OFDM signals," in *Proc. IEEE 26th Annu. Int. Symp. Pers., Indoor, Mobile Radio Commun. (PIMRC)*, Aug. 2015, pp. 271–275.
[13] T. Kageyama, O. Muta, and H. Gacanin, "Performance analysis of OFDM with peak cancellation under EVM and ACLR restrictions," *IEEE Trans. Veh. Technol.*, early access, Apr. 2, 2020, doi: 10.1109/TVT.2020.2982587.
[14] C. Studer and E. G. Larsson, "PAR-aware large-scale multi-user MIMO-OFDM downlink," *IEEE J. Sel. Areas Commun.*, vol. 31, no. 2, pp. 303–313, Feb. 2013.
[15] H. Bao, J. Fang, Z. Chen, H. Li, and S. Li, "An efficient Bayesian PAPR reduction method for OFDM-based massive MIMO systems," *IEEE Trans. Wireless Commun.*, vol. 15, no. 6, pp. 4183–4195, Jun. 2016.
[16] R. Zayani, H. Shaiek, and D. Roviras, "PAPR-aware massive MIMO-OFDM downlink," *IEEE Access*, vol. 7, pp. 25474–25484, 2019.

[17] H. Prabhu, O. Edfors, J. Rodrigues, L. Liu, and F. Rusek, "A low-complex peak-to-average power reduction scheme for OFDM based massive MIMO systems," in *Proc. 6th Int. Symp. Commun., Control Signal Process. (ISCCSP)*, May 2014, pp. 114–117.
[18] S. K. Mohammed and E. G. Larsson, "Per-antenna constant envelope precoding for large multi-user MIMO systems," *IEEE Trans. Commun.*, vol. 61, no. 3, pp. 1059–1071, Mar. 2013.
[19] J.-C. Chen, "Low-PAPR precoding design for massive multiuser MIMO systems via Riemannian manifold optimization," *IEEE Commun. Lett.*, vol. 21, no. 4, pp. 945–948, Apr. 2017.
[20] C. Ni, Y. Ma, and T. Jiang, "A novel adaptive tone reservation scheme for PAPR reduction in large-scale multi-user MIMO-OFDM systems," *IEEE Wireless Commun. Lett.*, vol. 5, no. 5, pp. 480–483, Oct. 2016.
[21] H. Bao, J. Fang, Q. Wan, Z. Chen, and T. Jiang, "An ADMM approach for PAPR reduction for large-scale MIMO-OFDM systems," *IEEE Trans. Veh. Technol.*, vol. 67, no. 8, pp. 7407–7418, Aug. 2018.
[22] M. Suzuki, T. Suzuki, Y. Kishiyama, and K. Higuchi, "Complexity-reduced algorithm for adaptive PAPR reduction method using null space in MIMO channel for MIMO-OFDM signals," in *Proc. 16th IEEE VTS Asia Pacific Wireless Commun. Symp.*, Aug. 2019, pp. 1–5.
[23] M. Suzuki, T. Suzuki, Y. Kishiyama, and K. Higuchi, "Method for generating peak cancellation signals in complexity-reduced PAPR reduction method using null space in MIMO channel for MIMO-OFDM signals," in *Proc. 16th IEEE VTS Asia Pacific Wireless Commun. Symp.*, Aug. 2019, pp. 1–5.
[24] A. Ivanov, A. Volokhatyi, D. Lakontsev, and D. Yarotsky, "Unused beam reservation for PAPR reduction in massive MIMO system," in *Proc. IEEE 87th Veh. Technol. Conf. (VTC Spring)*, Jun. 2018, pp. 1–5.
[25] T. Koike-Akino, P. Wang, and P. V. Orlik, "Joint lattice and subspace vector perturbation with PAPR reduction for massive MU-MIMO systems," in *Proc. IEEE Global Commun. Conf. (GLOBECOM)*, Dec. 2018, pp. 1–7.
[26] D. Tse and P. Viswanath, *Fundamentals of Wireless Communication*. Cambridge, U.K.: Cambridge Univ. Press, 2005.
[27] R. van Nee and A. de Wild, "Reducing the peak-to-average power ratio of OFDM," in *Proc. IEEE Veh. Technol. Conf.*, vol. 3, May 1998, pp. 2072–2076.

TOMOYA KAGEYAMA (Student Member, IEEE) received the B.E. and M.E. degrees from Kyushu University, Japan, in 2015 and 2017, respectively, where he is currently pursuing the Ph.D. degree. His research interests include PHY layer signal processing techniques for powerline communications and MIMO wireless communications.

OSAMU MUTA (Member, IEEE) received the B.E. degree from Ehime University, in 1996, the M.E. degree from the Kyushu Institute of Technology, Japan, in 1998, and the Ph.D. degree from Kyushu University, in 2001. In 2001, he joined the Graduate School of Information Science and Electrical Engineering, Kyushu University, as an Assistant Professor. Since 2010, he has been an Associate Professor with the Center for Japan-Egypt Cooperation in Science and Technology, Kyushu University. His current research interests include signal processing techniques for wireless communications and powerline communications, MIMO, and nonlinear distortion compensation techniques for high-power amplifiers. He is a Senior Member of the Institute of Electronics, Information and Communication Engineering (IEICE). He was a recipient of the 2005 Active Research Award in the IEICE Technical Committee of Radio Communication Systems and the Chairman's Award (Best Paper Award) from the IEICE Technical Committee of Communication Systems (2014, 2015, and 2017).

HARIS GACANIN (Senior Member, IEEE) received the Dipl.Ing. degree in electrical engineering from the University of Sarajevo, in 2000, and the M.Sc. and Ph.D. degrees from Tohoku University, Japan, in 2005 and 2008, respectively. He was with Tohoku University, from 2008 to 2010, first as the Japan Society for Promotion of Science Postdoctoral Fellow and later as an Assistant Professor. He joined Alcatel-Lucent (now Nokia), in 2010, where he worked as the Physical-Layer Expert, the Research Director, and the Department Head at Nokia Bell Labs until 2020. He is an Adjunct Professor with the University of Leuven (KU Leuven), Belgium, for the period of 2018–2020. He is currently a Full (Chair) Professor with RWTH Aachen University, Germany. His professional interests are related to broad areas of digital signal processing and artificial intelligence with applications in communication systems. He has more than 200 scientific publications (journals, conferences, and patent applications) and invited/tutorial talks. He is a Senior Member of the Institute of Electronics, Information and Communication Engineering (IEICE) and acted as the General Chair and Technical Program Committee Member of various IEEE conferences. He was a recipient of several Nokia innovation awards, the IEICE Communication System Study Group Best Paper Award (joint 2014, 2015, and 2017), The 2013 Alcatel-Lucent Award of Excellence, the 2012 KDDI Foundation Research Award, the 2009 KDDI Foundation Research Grant Award, the 2008 Japan Society for Promotion of Science (JSPS) Postdoctoral Fellowships for Foreign Researchers, the 2005 Active Research Award in Radio Communications, the 2005 Vehicular Technology Conference (VTC 2005-Fall) Student Paper Award from the IEEE VTS Japan Chapter, and the 2004 Institute of IEICE Society Young Researcher Award. He was awarded by Japanese Government (MEXT) Research Scholarship, in 2002. He is a Distinguished Lecturer of the IEEE Vehicular Technology Society and an Associate Editor of the *IEEE Communications Magazine*, while he served as an Editor for *IEICE Transactions on Communications* and *IET Communications*.